

The nonlinear stage in the growth of laser-induced periodic surface structures

L. A. Bol'shov, A. V. Moskovchenko, and M. I. Persiantsev

I. V. Kurchatov Atomic Energy Institute

(Submitted 16 July 1987)

Zh. Eksp. Teor. Fiz. **94**, 62–75 (April 1988)

We examine the nonlinear dynamics of the $\lambda / (1 \pm \sin\theta)$ gratings which dominate for p -polarization and the complementary $\lambda / 2$ grating, in the amplitude range from the initialization level to $h \sim (\zeta')^{1/2}\lambda$. In the process, we solve the multimode nonlinear diffraction problem. We show that in the nonlinear stage of growth, the $\lambda / 2$ grating exerts a significant influence on the development of the fundamental gratings.

1. INTRODUCTION

Numerous experiments (as reviewed in Ref. 1) have demonstrated that surface ripples can be produced in a variety of materials (including metals, semiconductors, and dielectrics) by high-power laser radiation. These ripples most frequently form one-dimensional gratings whose period is of the order of the incident wavelength λ , with their grooves oriented perpendicular to the field vector \mathbf{E}_0 . The linear stage of the growth of surface ripples has by now been thoroughly studied theoretically.²⁻⁴ In metals, for example, it is known that interference between the electromagnetic wave propagating through the medium and the surface-guided wave excited by surface irregularities will lead to the formation of ripples. Surface-guided waves play a dominant role in the formation of surface structures by virtue of the resonant nature of the way in which incident radiation is transformed into this wave, since for a fixed surface-relief amplitude, the conversion coefficient is larger by a factor ζ' than for other diffracted waves ($\zeta = \zeta' + i\zeta''$ is the surface impedance; for metals in the wavelength range 1–10 μm , typical values are $\zeta' \sim 10^{-2}$). We will therefore refer to those harmonics of the surface relief at which a surface-guided wave is excited in the first diffraction order as being resonant.

The linear stage of ripple growth comes to an end when the amplitude of the periodic surface relief is fairly low, $h \leq \zeta'\lambda$, and these structures still exercise a negligible influence on interactions between the laser beam and the surface. The nonlinear growth stage is considerably more interesting, being characterized by marked changes in surface absorptivity. Nonmonotonic growth of resonant gratings and the appearance of complementary gratings during the nonlinear growth stage have been noted in a number of experiments.⁵⁻⁸ For s -polarized pump waves, the first theoretical study of the nonlinear dynamics of ripple formation to a depth $h \sim \zeta'\lambda$ was reported in Ref. 9. Because of a methodological error, however, some of the important conclusions reached in that paper are incorrect. Specifically, it is not true that a stationary solution exists in the normal incidence case, where a resonant grating with spacing λ and a complementary grating with spacing $\lambda / 2$ are formed. We consider normal incidence below.

In the present paper, under conditions for which ripple formation results from laser-induced vaporization, we examine the nonlinear growth dynamics of resonant gratings with spacing $\lambda / (1 \pm \sin\theta)$ which are dominant for p -polarized incident radiation, and of the complementary grating with spacing $\lambda / 2$, both for amplitudes $h \sim (\zeta')^{1/2}\lambda$ which

exceed those detected in the experiment detailed in Ref. 10.

What we mean by a grating is a fairly compact group of resonant planar ripples in the surface relief, with central wave vectors lying in the plane of incidence. The angular width of such a group is determined by the intensity and geometry of the laser beam; under actual experimental conditions, this width would typically be 10–20° (Ref. 1). In our work, we treat the case in which the amplitudes $h_{\mathbf{k}}$ and phases $\varphi_{\mathbf{k}}$ of the planar ripples within a group are smooth functions of the deviation from the central wave vector \mathbf{k}_j , so that one can transform to amplitudes $\mathbf{h}_{\mathbf{k}_j}$ and phases $\varphi_{\mathbf{k}_j}$ averaged over each group:

$$h(\mathbf{r}) = \int |h_{\mathbf{k}}| \exp[i(\varphi_{\mathbf{k}} + \mathbf{k}\mathbf{r})] d\mathbf{k} = \sum_{j=1}^3 |h_{\mathbf{k}_j}| \exp[i(\varphi_{\mathbf{k}_j} + \mathbf{k}_j\mathbf{r})],$$

where \mathbf{r} is a two-dimensional vector lying in the plane of the surface. Groups of surface ripples then interact coherently.

A self-consistent examination of the nonlinear growth of resonant $\lambda / (1 \pm \sin\theta)$ gratings and the complementary $\lambda / 2$ grating requires that one take account of electrodynamic nonlinearities. The discussion of nonlinear effects is most conveniently based on expressions for the amplitude of surface-guided waves excited by a sinusoidal grating of amplitude h , as derived from a solution of the diffraction problem⁵.

$$H_{\text{SGW}} \sim khH_0 / [\zeta' + a(kh)^2],$$

where $k = 2\pi/\lambda$ is the wave vector of the light, H_0 is the incident wave amplitude, and a is a factor of order unity. It is clear from this expression that even for fairly small $h \sim \zeta'\lambda$, the amplitude of the excited surface wave can be comparable to H_0 , the amplitude of the pump wave. The interaction of counterpropagating surface waves leads to the formation of a $\lambda / 2$ grating (intermodal electrodynamic nonlinearity). There are, furthermore, unimodal electrodynamic nonlinearities associated with virtual multiple scattering of surface waves by resonant gratings when $h \sim (\zeta')^{1/2}\lambda$, and the resulting self-action of the gratings. Two similar scattering channels exist. In the first, a resonantly excited surface wave is virtually scattered into a specularly reflected wave, and then back into a surface wave. In the second, second-order diffraction waves act as intermediaries between virtual scattering events. The electrodynamic nonlinearities listed thus require that one solve the multimode nonlinear diffraction problem, taking second-order waves into account.

2. THE NONLINEAR DIFFRACTION PROBLEM

The problem we solve is that of a p -polarized plane wave diffracted by irregularities on a metallic surface which is represented by a combination of three gratings:

$$\begin{aligned} \xi(t, x) = & a(t) \exp[i\varphi_1(t) + iq_1x] \\ & + b(t) \exp[i\varphi_2(t) + iq_2x] + c(t) \exp[i\varphi_3(t) + i2kx] + \text{c.c.}, \end{aligned} \quad (1)$$

where $a(t)$ and $b(t)$ are the amplitudes of resonant gratings with wave vectors $q_{1,2} = (1 \mp \sin \theta)k$ respectively, and $c(t)$ is the amplitude of a grating with wave vector $2k$.

According to the Rayleigh method, the vacuum field may be written in the form

$$\begin{aligned} H = & H_0 \exp[i(k_1x + k_2z - \omega t)] + H_r \exp[i(k_1x - k_2z - \omega t)] \\ & + H_{(+)} \exp[i(kx - \omega t) + \Gamma z] + H_{(-)} \exp[-i(kx + \omega t) + \Gamma z] \\ & + H_1 \exp[i(k + q_1)x + \gamma_1z - i\omega t] + H_2 \exp[i(k + q_2)x \\ & + \gamma_2z - i\omega t] + H_3 \exp[-i(k + q_1)x + \gamma_1z - i\omega t] \\ & + H_4 \exp[-i(k + q_2)x + \gamma_2z - i\omega t] + H_5 \exp[i(3kx - \omega t) \\ & + 2^h kz] + H_6 \exp[-i(3kx + \omega t) + 2^h kz] \\ & + H_7 \exp[-i(k_1x + k_2z + \omega t)], \end{aligned} \quad (2)$$

in which the $H_{(\pm)}$ are the surface-wave amplitudes, H_r is the amplitude of the specular wave, H_{1-7} are the amplitudes of the second-order diffracted waves, $k_r = k \sin \theta$ is the tangential component of the incident wave vector, $\Gamma = (\zeta' + |\zeta''|)k$ is the normal component of the surface wave vector in vacuum, and

$$\gamma_1 = [(k + q_1)^2 - k^2]^{1/2}, \quad \gamma_2 = [(k + q_2)^2 - k^2]^{1/2}$$

are the normal components of the second-order wave vectors.

The scattered wave amplitudes are obtained from the Leontovich boundary condition with $z = \xi(t, x)$:

$$\frac{1}{k} [\mathbf{n}[\mathbf{kH}]] - \zeta(\mathbf{H} - \mathbf{n}(\mathbf{nH})) = 0, \quad (3)$$

where $\mathbf{n} = (\nabla_x \xi; 0; -1)[1 + (\nabla_x \xi)^2]^{-1/2}$ is the exterior unit normal. We then easily obtain a set of algebraic equations for the scattered wave amplitudes; these can clearly be solved as follows:

$$\begin{aligned} H_1 = \frac{k}{\gamma_1} q_1 a e^{i\varphi_1} H_{(+)}, \quad H_2 = \frac{k}{\gamma_2} q_2 b e^{i\varphi_2} H_{(+)}, \\ H_3 = \frac{k}{\gamma_1} q_1 a e^{-i\varphi_1} H_{(-)}, \quad H_4 = \frac{k}{\gamma_2} q_2 b e^{-i\varphi_2} H_{(-)}, \\ H_5 = \frac{kc}{2^{1/2}} e^{i\varphi_1} H_{(+)}, \quad H_6 = \frac{kc}{2^{1/2}} e^{-i\varphi_1} H_{(-)}, \\ H_7 = -i \frac{q_1 a}{\cos \theta} e^{i\varphi_1} H_{(-)} - i \frac{q_2 b}{\cos \theta} e^{-i\varphi_2} H_{(+)}, \\ H_r = \frac{\cos \theta - \zeta}{\cos \theta + \zeta} H_0 - i \frac{q_1 a}{\cos \theta} e^{-i\varphi_1} H_{(+)} - i \frac{q_2 b}{\cos \theta} e^{-i\varphi_2} H_{(-)}, \end{aligned} \quad (4)$$

where the amplitudes $H_{(\pm)}$ are given by

$$\begin{aligned} H_{(+)} = \frac{2i(g_2 b e^{-i\varphi_2} Q - q_1 a e^{i\varphi_1} P) H_0}{P^2 - QF}, \\ H_{(-)} = \frac{2i(q_1 a e^{i\varphi_1} F - q_2 b e^{-i\varphi_2} P) H_0}{P^2 - QF}, \end{aligned} \quad (5)$$

in which

$$\begin{aligned} P = & \zeta + i \frac{\Gamma}{k} + \frac{(q_1 a)^2 + (q_2 b)^2}{\cos \theta} - i \frac{k}{\gamma_1} (q_1 a)^2 \\ & - i \frac{k}{\gamma_2} (q_2 b)^2 - i 2^h (kc)^2, \end{aligned} \quad (6)$$

$$Q = 2 \left(\frac{q_1 a q_2 b}{\cos \theta} e^{i(\varphi_1 + \varphi_2)} + ikce^{i\varphi_1} \right),$$

$$F = 2 \left(\frac{q_1 a q_2 b}{\cos \theta} e^{-i(\varphi_1 + \varphi_2)} + ikce^{-i\varphi_1} \right).$$

Equations (4) and (5) solve the diffraction problem, as required for a self-consistent discussion of the growth of gratings to a depth $h \sim (\zeta')^{1/2} \lambda$. Higher-order diffracted waves are negligible, inasmuch as h/λ is a small parameter.

By using a surface profile of the form (1) to solve the diffraction problem, we have neglected the finite angular size $\Delta\beta$ of the groups of resonant surface ripples, and have assumed the scattered-wave polarization vectors to be coplanar. For $\Delta\beta \ll 1$, the error involved in this approximation is $(\Delta\beta)^2/2$. As we pointed out earlier, the magnitude of $\Delta\beta$ is governed by the angle of incidence θ and the degree to which the threshold for ripple formation has been exceeded. We can make use of the expression for the amplitude of the surface wave excited by the initialization grating h_β , and propagating at an angle β to the plane of incidence:

$$H_\beta = - \frac{2i(\cos \beta - \sin \theta) k h_\beta H_0}{\zeta + i\Gamma/k},$$

as well as the equation (A1.10) of Appendix 1 for ripple amplitude evolution in a periodic surface grating:

$$\dot{h}_\beta + \frac{T_0}{U} \chi q^2 h_\beta = \frac{Q_1(h_\beta)}{c_p U},$$

where χ , c_p are the thermal diffusivity and heat capacity of the metal, T_0 is the uniform component of the temperature, U is the specific heat of vaporization, and $Q = (c\zeta'/2\pi) \text{Re}\{\mathbf{H}_\beta \cdot \mathbf{H}_0^*\}$ is the inhomogeneous component of the absorbed thermal flux.¹⁾ One then easily obtains an expression for the rate corresponding to the initial stage of ripple growth:

$$\begin{aligned} \gamma = & \cos \beta (\cos \beta - \sin \theta) \frac{2\zeta' \Delta}{\Delta^2 + \zeta'^2} \gamma_p \\ & - (1 + \sin \theta - 2 \sin \theta \cos \beta) \nu, \end{aligned}$$

where $\Delta = (\Gamma/k) - |\zeta''|$, $\gamma_p = kJ_0/c_p U$, J_0 is the mean pump intensity, and $\nu = T_0 \chi k^2/U$.

We find from this expression, then, that the $\lambda/(1 - \sin \theta)$ grating has the lowest threshold intensity, $J_c = (1 - \sin \theta) k \chi T_0$. Significantly above threshold ($J_0 > J_c = 2k \chi T_0$), the $\lambda/(1 + \sin \theta)$ grating have the largest growth rate. The behavior of growth rate just above threshold ($J_0 \gtrsim J_c$) is shown as a function of the angle β in Fig. 1a. Positive growth rates are clearly localized to the range near $\cos \beta = 1$, corresponding to the $\lambda/(1 - \sin \theta)$ grating. At low angles of incidence ($\theta \leq 45^\circ$), the $\lambda/(1 + \sin \theta)$ grating ($\cos \beta = -1$) has the least attenuation ($\gamma < 0$). Figure 1b shows the angle dependence of the growth

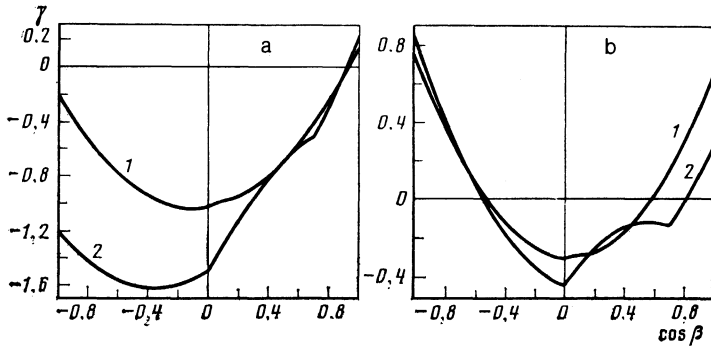


FIG. 1. a) Theoretical behavior of resonant grating growth rates γ as a function of their orientation, with periodically pulsed p -polarized pumping (curve 1 is for $\theta = 10^\circ$, curve 2 for $\theta = 45^\circ$). The growth rates γ are normalized to $\gamma_p = \tau_p \Omega k J_0 / c_p U (\lambda = 10 \mu\text{m}, J_0 = 3 \cdot 10^9 \text{ W/cm}^2, c_p U = 5 \cdot 10^4 \text{ J/cm}^3, \tau_p \Omega = 10^{-1}, T_{av} \approx 4 \cdot 10^3 \text{ K}, \chi = 0.1 \text{ cm}^2/\text{sec})$. b) Behavior of the resonant-grating growth rate γ as a function of its orientation when $\gamma \tau_p \gg 1$ (curve 1, $\theta = 10^\circ$; curve 2, $\theta = 45^\circ$).

rate well above threshold ($\gamma \tau_p \gg 1$). Here a fairly broad spectrum of harmonics of the surface relief is excited. If ripple development proceeds at a fairly low level ($h \ll \xi' \lambda$), however, then to the extent that it approaches the nonlinear development stage, the effects of harmonics at large angles β from the plane of incidence will be mitigated. The principal contribution will come from harmonics near the local maximum of the growth rate at $\cos \beta = \pm 1$. Our analysis of the linear stage of grating development thus makes it possible to identify a range of laser beam parameters for which the $\lambda / (1 \pm \sin \theta)$ gratings which are formed, at least in an approximation to the nonlinear stage, are made up of compact groups of surface harmonics ($\Delta \beta \ll 1$). The approximation used to solve the diffraction problem for this case will then be valid. In an actual experimental situation, the error induced by the scalar approximation lies within a range of a few percent ($(\Delta \beta)^2 \lesssim 0.06$).

3. NONLINEAR DYNAMICS OF THE GROWTH OF INTERACTING GRATINGS

Grating growth during laser vaporization is governed by the corresponding spatial components of the absorbed thermal flux; these form the basis for the expressions for the scattered wave fields (4) and (5):

$$Q_1 = \frac{c \xi'}{4\pi} \{ [(H_0^* + H_7^*) H_{(+)} + H_1 H_{(+)}^* + H_3^* H_{(-)} + H_7 H_{(-)}^*] e^{i q_1 x} + [(H_0 + H_7) H_{(-)}^* + H_2 H_{(+)}^* + H_7^* H_{(+)} + H_4^* H_{(-)}] e^{i q_2 x} + [H_{(+)} H_{(-)}^* + H_5 H_{(+)}^* + H_6^* H_{(-)}] e^{2i k x} + \text{c.c.} \} \quad (7)$$

The dynamical equations for the grating amplitudes $a(t)$, and $c(t)$ and the spatial phase $\Phi(t) = \varphi_3 - \varphi_1 - \varphi_2$ are obtained by substituting (7) into (A1.10). The complete set of dynamical equations valid to a grating depth of $h \sim (\xi')^{1/2} \lambda$ is fairly complicated, and we relegate it to Appendix 2.

Here we present the dynamical equations which hold in the approximation $h \ll (\xi')^{1/2} \lambda$:

$$\begin{aligned} \dot{x} + v_1 x &= P_1 [x(1 - 2z^2) + 2(\sin \Phi + 2z^2 \cos \Phi) y z], \\ \dot{y} + v_2 y &= P_2 [y(1 - 2z^2) + 2(-\sin \Phi + 2z^2 \cos \Phi) x z], \\ \dot{z} + v_3 z &= -x y (1 + 2z^2) \cos \Phi + (x^2 + y^2) z, \\ \dot{\Phi} &= 2 \operatorname{tg} \theta (1 + 2z^2) + y^2 - x^2 + \frac{x y}{z} (1 - 2z^2) \sin \Phi \\ &+ 2P_1 \frac{y z}{x} (\cos \Phi - 2z^2 \sin \Phi) - 2P_2 \frac{x z}{y} (\cos \Phi + 2z^2 \sin \Phi), \end{aligned} \quad (8)$$

where

$$\begin{aligned} x &= \frac{q_1 a}{\xi' \cos^2 \theta}, & y &= \frac{q_2 b}{\xi' \cos^2 \theta}, & z &= \frac{k c}{\xi'}, \\ P_{1,2} &= \frac{1 \pm \sin \theta}{\cos \theta}, & v_1 &= \frac{(1 - \sin \theta)^2}{\cos \theta} \frac{k \kappa T_0}{J_0}, \\ v_2 &= \frac{(1 + \sin \theta)^2}{\cos \theta} \frac{k \kappa T_0}{J_0}, & v_3 &= \frac{4 k \kappa T_0}{J_0}, \end{aligned}$$

and differentiation is performed with respect to

$$\tau = \int_0^t \frac{dt'}{W_1^2 + W_2^2}$$

(see Appendix 2).

Let us consider the behavior of the solution of (8) in certain asymptotic ranges of the variables x , y , and z .

a) *Initial stage* ($x, y, z < 1$). In this region, the solution is of the form

$$\begin{aligned} x &= x_0 \exp[(P_1 - v_1)t], & y &= y_0 \exp[(P_2 - v_2)t], \\ z e^{i \Phi} &= z_0 e^{i \Phi_0} \exp[-(v_3 + 2i \operatorname{tg} \theta)t] \\ &- \frac{x_0 y_0 \exp[(P_1 + P_2 - v_1 - v_2)t]}{P_1 + P_2 - v_1 - v_2 + v_3 + 2i \operatorname{tg} \theta}. \end{aligned}$$

Clearly, when the difference in the rate of growth in x and y is small ($P_1 - v_1 \approx P_2 - v_2$) and the initial amplitudes are equal ($x_0 = y_0$), the variables x , y , and z all attain values of the order of unity simultaneously, the growth in z being determined by the spatial phase Φ . If the initial phase is such as to make the nonlinear feedback from x and y and z negative and damp z , then the main term in the equation for the phase (at least from some time onward) will be the one with z in the denominator. This induces a change in the phase which ensures that x and y will feed back positively to z , with z increasing as a consequence. This interaction process, wherein the phase is maintained near a certain value providing optimal conditions for the growth of the least of the three gratings, is known as phase localization.¹²

b) *The large-amplitude case* ($x, y, z > 1$) In this limit, the dynamic equations become conservative:

$$\begin{aligned} \dot{x} &= y z^3 \cos \Phi, & \dot{y} &= x z^3 \cos \Phi, \\ \dot{z} &= -x y z^2 \cos \Phi, & \dot{\Phi} &= -\left(x y z + \frac{y z^3}{x} + \frac{x z^3}{y}\right) \sin \Phi. \end{aligned} \quad (8')$$

Here we have transformed variables:

$$P_2^{1/2}x \rightarrow x, \quad P_1^{1/2}y \rightarrow y, \quad 2^{1/2}z \rightarrow z, \quad 2^{1/2}\tau \rightarrow \tau.$$

Integrals of the motion for the system (8') take the form

$$x^2 + z^2 = M_1, \quad y^2 + z^2 = M_2, \quad x^2 y^2 \sin^2 \Phi / z^2 = S. \quad (9)$$

The existence of such integrals of the motion enables us to transform to the following set of equations:

$$(\dot{x})^2 + \pi_1(x) = 0, \quad (\dot{y})^2 + \pi_2(y) = 0, \quad (\dot{z})^2 + \pi_3(z) = 0, \quad (10)$$

where

$$\pi_1(x) = (M_1 - x^2)^4 (S/x^2 + 1) - M_2 (M_1 - x^2)^3,$$

$$\pi_2(y) = (M_2 - y^2)^4 (S/y^2 + 1) - M_1 (M_2 - y^2)^3,$$

$$\pi_3(z) = S z^6 - z^4 (M_1 - z^2) (M_2 - z^2),$$

and to investigate the behavior of the solutions using nonlinear potential theory: curves showing the potentials $\pi_1(x)$, $\pi_2(y)$, and $\pi_3(z)$ are shown in Fig. 2. Here we must point out that values $z < 1$ correspond to the stationary points $x(t)$, $y(t)$, and that the large-amplitude approximation breaks down in this region, with the system of equations ceasing to be conservative. For $z > 1$, the system executes conservative oscillations, with the maxima of z corresponding to the minima of x and y ; the minima of z are less than unity. There are segments of the x and y trajectories near the minima of z that correspond to regions of exponential growth in x and y , since the coupling between them through z is small, while the inherent nonlinearity is still negligible. In this respect, the behavior of trajectories near the minima of z is similar to that in the initial stage, although since x and y are large, phase localization and the nonlinear growth in z are more abrupt.

We consider the case of normal incidence ($\theta = 0^\circ$, $x \equiv y$) separately:

$$\begin{aligned} \dot{x} + v_1 x &= x(1 - 2z^2) + 4xz^3 \cos \Phi, \\ \dot{z} + v_3 z &= -x^2(1 + 2z^2) \cos \Phi + 2x^2 z, \\ \dot{\Phi} &= [(x^2/z)(1 - 2z^2) - 4z^3] \sin \Phi. \end{aligned} \quad (11)$$

It can be shown that just above threshold ($\varepsilon = 1 - v_1 \ll 1$), (11) has the following stable stationary solution:

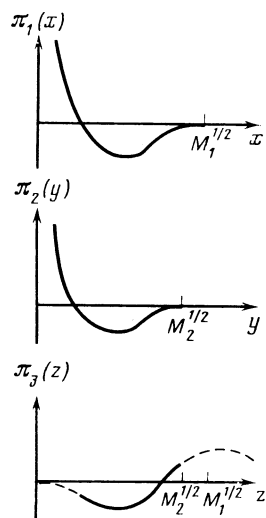


FIG. 2.

$$X_0 = v_3 \left(\frac{1 - v_1}{2} \right)^{1/2}, \quad Z_0 = \left(\frac{1 - v_1}{2} \right)^{1/2}, \quad \Phi_0 = \pi.$$

When the system is in fact well above threshold ($v \ll 1$), (11) has no stationary solutions. In the region $x, z > 1$, the system executes nonlinear oscillations as described above. Gandel'man and Kondratenko,⁹ arbitrarily putting $\Phi = -\pi$ in (11), came to the mistaken conclusion that the system has a stationary solution in the weak damping case, with a zero-amplitude λ -spaced grating (that is, $X_0 = 0, \dot{X}_0 = 0$) and a finite-amplitude $\lambda/2$ -spaced grating ($Z_0 \sim 1, \dot{Z}_0 = 0$).

4. DISCUSSION AND SUMMARY

A numerical solution of the full set of dynamic equations A2.1 is consistent with the qualitative behavior discussed above for the trajectories $x(t)$, $y(t)$, $z(t)$. For example, Fig. 3 shows the computed results for normal incidence in the initial stage of growth. Here the grating amplitudes start from $h \ll \xi' \lambda$ and grow all the way to $h \sim \xi' \lambda$. Phase localization in the vicinity of π and the consequent nonlinear growth in z are clearly evident. In the nonlinear stage, the behavior of the grating amplitudes depends strongly on how far above threshold the system is operating. Just above threshold, when only the x -grating grows exponentially in the initial stage, the system behaves as follows (see Fig. 4). When the x values are of order unity ($h \sim \xi' \lambda$), the y - and z -gratings start to develop, due to a dissociation instability in x . The system proceeds to execute several damped oscillations, and finally reaches the steady state, with the stationary x -value being greater than the stationary y - and z -values. The stationary grating amplitudes are at a level $h \sim \xi' \lambda$.

When the threshold is exceeded by a considerable amount, y can exhibit a large growth rate compared with x , and can outstrip x in the initial stage (see Fig. 5). The phase will therefore be localized around values for which the nonlinear coupling between x and z is positive, but between x and y it is negative. The net result is that x outpaces y when $x, y, z \sim 1$. The theoretically predicted occurrence of an integral

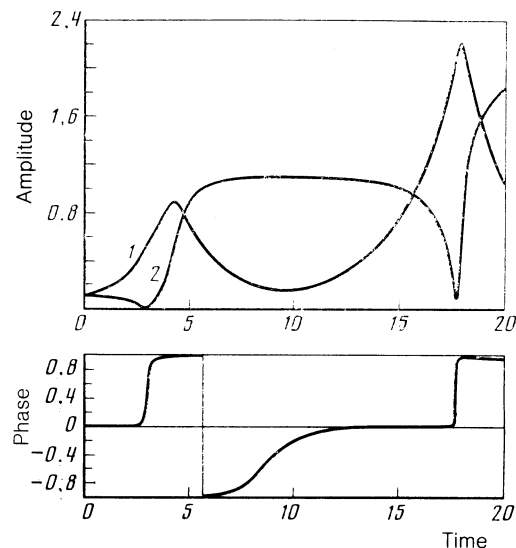


FIG. 3. The initial stage of growth of periodic surface relief (normal incidence). Grating amplitude values are normalized to $\xi' \lambda$; the unit of time is $(2\gamma_p)^{-1}$.

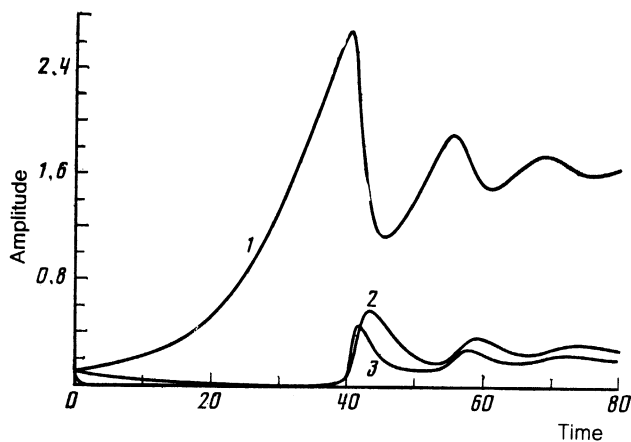


FIG. 4. Evolution of the dominant gratings under p -polarized pulsed periodic illumination. Grating amplitudes are normalized to $\xi'\lambda$, and the unit of time is $(2\gamma_p)^{-1}$. The angle of incidence θ is 10° (curve 1: $\lambda/(1 - \sin \theta)$; curve 2: $\lambda/(1 + \sin \theta)$; curve 3: $\lambda/2$).

of the type $x^2 - y^2 = \text{const}$ in a system with almost conservative behavior will dictate the predominance of x over y beyond that region as well, and this is also consistent with the calculations. Furthermore, a numerical treatment enables one to track the approach of the maximum x - and y -values to the steady state engendered by an inherent nonlinearity ($h \sim (\xi')^{1/2}\lambda$), with the steady-state nonlinear oscillation stage near the maximum values being insensitive to the choice of initial conditions (our calculations were carried out with initial values $x, y, z \sim 0.01-0.1$).

Our qualitative analytic study of the system of equations (8) and numerical calculations using the full dynamical system enable us to make the following statements.

1) Notwithstanding the conclusions of Ref. 4, there is an intensity threshold associated with the production of periodic surface structures by pulsed periodic excitation which is related to the equalization of temperature differences by thermal diffusion between one pulse and the next. The $\lambda/(1 - \sin \theta)$ grating has the minimum mean threshold intensity (see Fig. 1a).

2) The exponential growth of the $\lambda/(1 \pm \sin \theta)$ gratings is accompanied by nonlinear growth of the complementary $\lambda/2$ grating. With normal incidence, the λ and $\lambda/2$ gratings reach a depth $h \sim \xi'\lambda$ practically simultaneously, and the spatial phase shift between gratings is exactly π at finite times (see Fig. 3). The system of gratings behaves similarly under oblique incidence of the pump beam as well.

3) Just above threshold, the $\lambda/(1 - \sin \theta)$ grating may be the only one with a positive growth rate. The $\lambda/(1 + \sin \theta)$ and $\lambda/2$ gratings begin to grow, due to a dissociation instability of the $\lambda/(1 - \sin \theta)$ grating after the latter reaches a depth $h \sim \xi'\lambda$. The grating amplitudes reach steady-state values $h \sim \xi'\lambda$, with the $\lambda/(1 - \sin \theta)$ grating being the most pronounced (see Fig. 4).

4) Well above threshold, the amplitudes of the principal gratings grow to a depth $h \sim (\xi')^{1/2}\lambda$ and perform in-phase oscillations about that value; the amplitude of the $\lambda/2$ grating oscillates in antiphase with the other two, at a level $h \sim \xi'\lambda$. Saturation of the principal grating amplitudes results from their intrinsic combined nonlinearity. The presence of a complementary grating is the decisive factor in determining which of the principal gratings will dominate when they saturate in amplitude. The concomitant growth of the gratings may result in the grating which dominates the nonlinear stage not being the one with the greatest growth rate (see Fig. 5).

5. CONCLUSION

In closing, we wish to discuss the relationship between our results and the published experimental data. Even though the nonlinear stage in the growth of periodic surface ripples has not yet been thoroughly investigated experimentally, there are a number of experimental factors suggesting that our theoretical model is consistent with reality. One example is the ripple production threshold observed experimentally with pulsed periodic laser excitation (see Ref. 11). Keilmann and Bai¹³ and Ursu *et al.*¹⁴ have detected an intermediate growth stage in the λ -spaced grating in which the sinusoidal shape of the grooves is distorted; this takes place when the grating amplitude is still rather small. Unfortunately, these authors do not cite any experimental data taken at oblique incidence ($\theta \neq 0$). It ought to be possible to use these data to establish whether the distortion of the sinusoidal shape of the grating is due to the nonlinearity of the thermophysical mechanism or the formation of the $\lambda/2$ grating. Bazhenov *et al.*¹⁵ indicate that they have observed the $\lambda/2$ grating (with $\theta \neq 0$) by means of its reflected diffraction pattern, but they do not provide the corresponding photographs. A number of authors have observed nonmonotonic growth of the principal gratings, in both single-pulse mode (well above the ripple production threshold)⁶ and pulsed periodic mode,^{7,8} but ripple production in these experiments was not due to vaporization. Even though our present treatment of the nonlinear stage of grating behavior relies largely on an electrodynamic nonlinearity, an extension of these re-

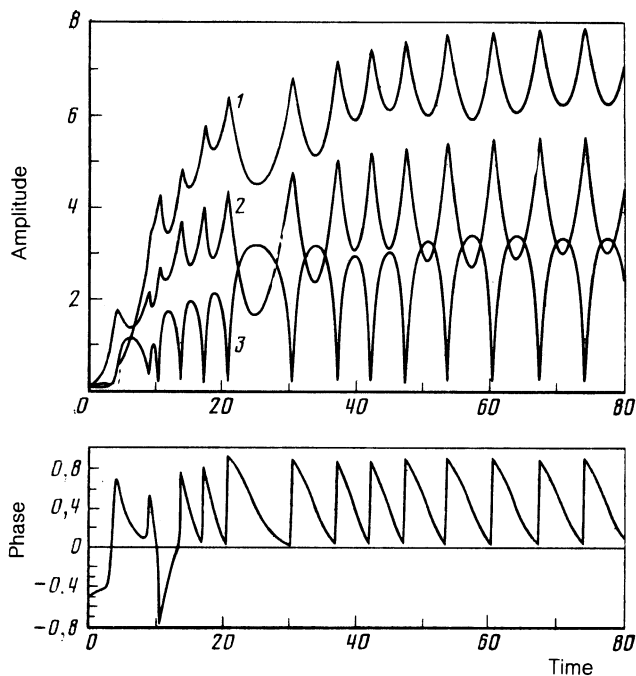


FIG. 5. Evolution of the dominant gratings under p -polarized illumination with $\gamma\tau_p \gg 1$. Grating amplitudes are normalized to $\xi'\lambda$ and the unit of time is $(2\gamma_p)^{-1}$. Angle of incidence θ is 10° (curve 1: $\lambda/(1 - \sin \theta)$; curve 2: $\lambda/(1 + \sin \theta)$; curve 3: $\lambda/2$).

sults to any other growth mechanism requires a certain amount of caution and further investigation.

APPENDIX 1

We consider laser-induced vaporization as the thermo-physical basis for the growth of periodic surface structures. In Ref. 4, Emel'yanov *et al.* discussed the initial stage of ripple formation when $\gamma\tau_p \ll 1$ (γ is the growth rate and τ_p is the laser pulse duration). This corresponds to ripple formation well above threshold. Here we adapt these arguments to the nonlinear problem. In addition, we examine the grating dynamics for the case in which a pulse is made up of a series of subpulses (mode-locking), with $\gamma\tau_p \ll 1$ (τ_p here is the duration of a subpulse). It is then possible for a beam just above threshold to produce ripples. The existence of a production threshold results from the equalization of thermal inhomogeneities through thermal diffusion in the time between subpulses. Both modes of ripple growth ($\gamma\tau_p \gg 1$ and $\gamma\tau_p \ll 1$) have been observed experimentally.¹

Let a metal occupy the semi-infinite space $z \gg \xi(t, x)$, with a thermal flux

$$Q = Q_0(t) + \sum_q [Q_q(t) e^{iqx} + \text{c.c.}]$$

being absorbed at the boundary (the summation is over the harmonics of the thermal flux distribution corresponding to the dominant gratings). We shall assume that the parameters of the laser beam interaction are such that we can neglect gas-phase processes above the surface.¹⁶ The surface heating and vaporization problem then reduces to the thermal diffusion equation in the metal:

$$\dot{T} = \chi \Delta T \quad (\text{A1.1})$$

$$\xi - \frac{\chi}{U} \frac{\partial T}{\partial n} = \frac{Q}{c_p U}, \quad \xi = C_0 e^{-U/T}$$

at $z = \xi(t, x)$, where C_0 is a constant which is roughly equal to the speed of sound in the metal ($C_0 \approx 3 \cdot 10^5$ cm/sec. With the change of variables $x' \equiv x$, $t' \equiv t$, $z' = z - \xi(t, x)$, Eq. (A1.1) gives

$$T - \xi \frac{\partial T}{\partial z'} = \chi \left[\Delta T - 2\xi_{x'} \frac{\partial^2 T}{\partial x \partial z'} - \xi_{xx''} \frac{\partial T}{\partial z'} + (\xi_{x'}')^2 \frac{\partial^2 T}{\partial z'^2} \right] \quad (\text{A1.2})$$

with boundary conditions

$$\xi - \frac{\chi}{U} \frac{\partial T}{\partial z'} = \frac{Q}{c_p U}, \quad (\text{A1.3})$$

$$\xi = C_0 \exp\left(-\frac{U}{T}\right) \quad (\text{A1.4})$$

at $z' = 0$. Equation (A1.3) is the condition for thermal flux balance at the boundary; it can further be used to derive the dynamic equations for the gratings. We will be interested in the situation where the thermal diffusion flux in (A1.3) can be neglected; the vaporization rate will then be determined by the absorbed flux Q . The dynamics of the spatially nonuniform surface relief will thus, in general, be governed by the nonlinear dependence of the absorbed flux on its amplitude. We have in mind here electrodynamic nonlinearities, as dis-

cussed above. Thermal diffusivity manifests itself in the grating dynamics as damping, which is important when $\gamma\tau_p \ll 1$ due to the gaps between pulses. Equation (A1.4) describes the kinetics of vaporization within the scope of the model detailed in Ref. 16. We seek a solution of (A1.2) in the form

$$T(t, x, z') = T_0(t, z') + \sum_q [T_q(t, z') e^{iqx} + \text{c.c.}]$$

and

$$\dot{\xi}(t, x) = v_0(t) + \sum_q [\dot{h}_q(t) e^{iqx} + \text{c.c.}],$$

where v_0 is the uniform speed at which the vaporization front moves, and

$$h(t, x) = \sum_q [h_q(t) e^{iqx} + \text{c.c.}]$$

specifies the spatially periodic surface relief. The thermal problem can be framed in terms of its Fourier components; we rewrite Eq. (A1.2) and the boundary conditions (A1.3) and (A1.4) after Fourier transformation:

$$T_q - v_0(t) \frac{\partial T_q}{\partial z'} - (\dot{h}_q + \chi q^2 h_q) \frac{\partial T_0}{\partial z'} = \chi \left(\frac{\partial^2 T_q}{\partial z'^2} - q^2 T_q \right), \quad (\text{A1.2}')$$

and at $z' = 0$,

$$h_q - \frac{\chi}{U} \frac{\partial T_q}{\partial z'} = \frac{Q_q}{c_p U}, \quad (\text{A1.3}')$$

$$\dot{h}_q = \int v_0(t) \exp\left(-iqx + \frac{UT}{T_0}\right) dx, \quad (\text{A1.4}')$$

where

$$v_0(t) = C_0 \exp\left(-\frac{U}{T_0(t)}\right), \quad T' = \sum_q [T_q(t, 0) e^{iqx} + \text{c.c.}]$$

is the spatially nonuniform surface temperature distribution. Note that we intentionally left out the nonlinear terms in Eq. (A1.2'); these are shown below to be small compared with the linear terms. We first consider the case in which the system is well above the threshold for producing periodic surface structures ($\gamma\tau_p \gg 1$).

a) *Initial stage of growth.* We assume that a stationary vaporization wave is established by surface heating during a pulse ($\tau_p \gg \chi/v_0^2$). Then

$$T_0(z') = T_0 \exp\left(-\frac{v_0 z'}{\chi}\right), \quad v_0 \approx \frac{Q_0}{c_p U}.$$

A solution of Eq. (A1.2') of the form $T_q(t, z') = T_q(z') e^{\gamma t}$ which satisfies the linearized version of the boundary condition (A1.4'),

$$\dot{h}_q = v_0 U T_q / T_0^2,$$

will take the form

$$T_q = \left[\left(\frac{v_0}{\chi} + \frac{\gamma T_0}{v_0 U} \right) e^{-sz'} - \frac{v_0}{\chi} e^{-v_0 z'/\chi} \right] h_q T_0,$$

$$g = \frac{v_0}{2\chi} + \left[\left(\frac{v_0}{2\chi} \right)^2 + \frac{\gamma}{\chi} + q^2 \right]^{1/2}, \quad \text{Re } q > 0.$$

Substituting the solution thus obtained into (A1.3'), and bearing in mind that $Q_q = qJ_0 h_q$ in the initial growth stage,

leads to an expression for the growth rate. In the parameter range under consideration,

$$v_0 \gg (\chi q / 4 \zeta') (T_0 / U)^4, \quad (\text{A1.5})$$

the expression for the growth rate is of the form

$$\dot{\gamma} = q J_0 / c_p U - \nu, \quad (\text{A1.6})$$

where the damping ν induced by the thermal diffusivity is much lower than the pump factor $\gamma_p = q J_0 / c_p U \equiv q v_0 / 4 \zeta'$. We use the expression for the damping ν below when we consider ripple production just above threshold.

b) The nonlinear stage of growth. In the nonlinear stage of grating growth $|Q_q| \sim Q_0$, so if we write (A1.3') in the analytically more tractable form

$$\dot{h}_q = \frac{Q_q}{Q_0} v_0 + \frac{\chi}{U} \frac{\partial T_q}{\partial z'},$$

we have $|h_q| \sim v_0$, and the thermal problem becomes nonlinear by virtue of the boundary condition (A1.4'). The inequality (A1.5), however, enables one to neglect the thermal nonlinearity, which appears in the thermal diffusion term of (A1.3'), by comparison with the electrodynamic term. Based on (A1.3'), then, the evolution equation for spatially periodic surface relief takes the form

$$\dot{h}_q = Q_q / c_p U. \quad (\text{A1.7})$$

We next examine the growth of periodic surface structures induced by a laser beam with temporal structure typical of mode-locked operation. We shall assume that the average surface heating produced by the laser is sufficient to induce well-developed vaporization ($\tau^* \ll \chi / v_{av}, v_{av} \approx 4 \zeta' J_{av} / c_p U, \tau^*$ is the length of interaction, $J_{av} = \tau_p \Omega J_0$ is the mean intensity, Ω is the subpulse repetition rate). The spatially periodic surface relief is enhanced during each subpulse, while thermal diffusion-induced equalization of temperature irregularities and attenuation of the grating amplitudes takes place more slowly, in the intervals between subpulses. Under these circumstances, then, it only makes sense to speak of a rate of grating growth averaged over many subpulses.

Using (A1.3'), we now derive an equation describing the average growth of ripples. During each subpulse, thermal balance is maintained at the surface between the pump radiation (as manifested in the absorbed flux) and the response of the medium (as manifested in nonuniform vaporization); between subpulses, thermal diffusion-induced grating attenuation takes place. The expression for the thermal diffusion flux comes from the balance condition obtained by integrating (A1.2') from zero to infinity:

$$-\chi T_q' = (\dot{h}_q + \chi q^2 h_q) T_0 + v_0 T_q + \int_0^\infty (T_q + \chi q^2 T_q) dz'. \quad (\text{A1.8})$$

Here we note that the nonlinear terms previously left out of the derivation of (A1.2') make a negligible contribution to the right-hand side of (A1.8), of the order of $(\dot{h}_{q-k} + \chi q^2 h_{q-k}) T_k$ (since $|T_k| \ll T_0$). Furthermore, (A1.8) can be transformed to the simpler form

$$-\chi T_q' = (\dot{h}_q + \chi q^2 h_q) T_0 \quad (\text{A1.9})$$

by using the linearized condition (A1.4'), and some simple estimates which allow for the fact that just above threshold $|\dot{h}_q| \lesssim \chi q^2 |h_q|$. Substituting the average thermal diffusion flux and pump beam into (A1.3'), we obtain the dynamic equation

$$\dot{h}_q + \frac{T_0}{U} \chi q^2 h_q = \tau_p \Omega \frac{Q_q}{c_p U}. \quad (\text{A1.10})$$

This implies that in the initial growth stage, growth rate is given by

$$\gamma = \frac{\tau_p \Omega q J_0}{c_p U} - \frac{T_0}{U} \chi q^2. \quad (\text{A1.11})$$

It is clear from (A1.11) that the system can be slightly above threshold for production of periodic surface structures when $J_{av} \gtrsim q \chi c_p T_0$. If $\gamma \tau_p \gg 1$, the analogous expression for low attenuation ($\nu = T_0 \chi q^2 / U$) is valid for $v_0 \gg \chi q T_0 / 4 \zeta' U$.

APPENDIX 2

We present here the complete set of dynamic equations; for convenience, we use the same variables as in (8):

$$\begin{aligned} \dot{x} + v_1 x &= P_1 \{ G_2 W_2 - G_1 W_1 \\ &\quad - \zeta' dx (G_1^2 + G_2^2 + U_1^2 + U_2^2) \} (W_1^2 + W_2^2)^{-1}, \\ \dot{y} + v_2 y &= P_2 \{ U_2 W_2 - U_1 W_1 \\ &\quad - \zeta' gy (G_1^2 + G_2^2 + U_1^2 + U_2^2) \}; W_1^2 + W_2^2)^{-1}, \\ \dot{z} + v_3 z &= - \{ (G_1 U_1 + G_2 U_2) \cos \Phi + (G_1 U_2 - G_2 U_1) \sin \Phi + 2^{-1/2} \zeta' z \\ &\quad \cdot (G_1^2 + G_2^2 + U_1^2 + U_2^2) \} (W_1^2 + W_2^2)^{-1}, \quad (\text{A2.1}) \\ \dot{\Phi} &= \{ [(G_1 U_1 + G_2 U_2) \sin \Phi + (G_2 U_1 - G_1 U_2) \cos \Phi] / z \\ &\quad - (G_1 W_2 + G_2 W_2) P_1 / x - (U_1 W_2 + U_2 W_1) P_2 / y + (2 \zeta' / \cos \theta) \\ &\quad \cdot (G_1^2 + G_2^2 - U_1^2 - U_2^2) \} (W_1^2 + W_2^2)^{-1}, \end{aligned}$$

where differentiation is with respect to $\tau = 2k J_0 t / c_p U$;

$$\begin{aligned} W_1 &= [1 + \zeta' (x^2 + y^2)]^2 - [1 - \zeta' (dx^2 + gy^2 + \sqrt{2} z^2)]^2, \\ W_2 &= 2 [1 + \zeta' (x^2 + y^2)] [1 - \zeta' (dx^2 + gy^2 + \sqrt{2} z^2)] - 8 \zeta' xyz \cos \Phi, \\ G_1 &= x [1 - \zeta' (dx^2 + gy^2 + \sqrt{2} z^2)] - 2yz \cos \Phi, \\ G_2 &= x [1 + \zeta' (x^2 - y^2)] + 2yz \sin \Phi, \\ U_1 &= y [1 - \zeta' (dx^2 + gy^2 + \sqrt{2} z^2)] - 2xz \cos \Phi, \\ U_2 &= y [1 - \zeta' (x^2 - y^2)] - 2xz \sin \Phi, \\ d &= \frac{\cos \theta}{[(2 - \sin \theta)^2 - 1]^{1/2}}, \quad g = \frac{\cos \theta}{[(2 + \sin \theta)^2 - 1]^{1/2}}. \end{aligned}$$

¹⁾ We note that when a surface-guided wave is generated, the calculated heat release in the impedance approximation differs from that computed using the volume formulas. Here we have used the exact volume formulas of Ref. 11.

¹A. E. Siegman and P. M. Fauchet, IEEE J. Quant. Electr. **QE-22**, 1384 (1985).

²S. A. Akhmanov, V. I. Emel'yanov, N. I. Koroteev, and V. N. Seminogov, Usp. Fiz. Nauk **147**, 675 (1985) [Sov. Phys. Usp. **28**, 1084 (1985)].

³V. I. Emel'yanov and V. N. Seminogov, Zh. Eksp. Teor. Fiz. **86**, 1026 (1984) [Sov. Phys. JETP **59**, 598 (1984)].

⁴V. I. Emel'yanov, E. M. Zemskov, and V. N. Seminogov, Kvant. Elektron. (Moscow) **11**, 2283 (1984) [Sov. J. Quantum Electron. **14**, 1515 (1984)].

- ⁵V. N. Anisimov, V. F. Baranov, L. A. Bol'shov, *et al.*, *Poverkhnost'*, No. 7, 138 (1983).
- ⁶F. Keilmann, *Phys. Rev. Lett.* **51**, 2097 (1983).
- ⁷J. F. Young, J. S. Preston, J. E. Sipe, and H. M. van Driel, *Phys. Rev.* **B27**, 1424 (1983).
- ⁸A. M. Prokhorov, V. A. Sychugov, A. V. Tishchenko, and A. A. Khakimov, *Pis'ma Zh. Tekh. Fiz.* **8**, 1409 (1982) [*Sov. Tech. Phys. Lett.* **8**, 605 (1982)]; *Pis'ma Zh. Tekh. Fiz.* **9**, 69 (1983) [*Sov. Tech. Phys. Lett.* **9**, 29 (1983)].
- ⁹G. M. Gandel'man and P. S. Kondratenko, *Zh. Eksp. Teor. Fiz.* **88**, 1470 (1985) [*Sov. Phys. JETP* **61**, 880 (1985)].
- ¹⁰V. N. Anisimov, V. P. Kozolupenko, A. Yu. Sebrant, and M. A. Stepanov, *Tezisy dokladov mezhotraslevoi nauchno-tekhnicheskoi konferentsii po vzaimodeistviyu izlucheniya plazmennykh i elektronnykh puchkov veshchestvom* (Abstracts of Papers, Interdivisional Scientific and Technical Conference on the Interaction of Radiation from Plasma and Electron Beams with Matter), TsNIIatominform, Moscow (1984), p. 77.
- ¹¹L. D. Landau and E. M. Lifshits, *Elektrodinamika sploshnykh sred*, Nauka, Moscow (1982), pp. 379, 430 [*Electrodynamics of Continuous Media*, Pergamon, Oxford (1984)].
- ¹²J. Weiland and H. Wilhelmsson, *Coherent Nonlinear Interaction of Waves in Plasma*, Pergamon, New York (1977).
- ¹³F. Keilmann and Y. H. Bai, *Appl. Phys. A* **29**, 9 (1982).
- ¹⁴I. Ursu, I. N. Mihailescu, L. C. Nistor, *et al.*, *Appl. Opt.* **24**, 3736 (1985).
- ¹⁵V. V. Bazhenov, A. M. Bonch-Bruевич, M. N. Libenson, and V. S. Makin, *Pis'ma Zh. Tekh. Fiz.* **10**, 1520 (1984) [*Sov. Tech. Phys. Lett.* **10**, 642 (1984)].
- ¹⁶S. I. Anisimov, *Zh. Eksp. Teor. Fiz.* **54**, 339 (1968) [*Sov. Phys. JETP* **27**, 182 (1968)].

Translated by M. Damashek